



Rapamycin and Resveratrol Modulate the Gliotic and Pro-Angiogenic Response in Müller Glial Cells Under Hypoxia

Paula V. Subirada^{1,2}, María V. Vaglianti^{1,2}, Mariana B. Joray^{3,4}, María C. Paz^{1,2†}, Pablo F. Barcelona^{1,2} and María C. Sánchez^{1,2*}

OPEN ACCESS

Edited by:

Nathan Anthony Smith,
Children's National Hospital,
United States

Reviewed by:

Ana Raquel Santiago,
University of Coimbra, Portugal
Paola Bagnoli,
University of Pisa, Italy

*Correspondence:

María C. Sánchez
maria.cecilia.sanchez@unc.edu.ar

†Present address:

María C. Paz,
Consejo Nacional de Investigaciones
Científicas y Técnicas (CONICET),
Unidad de Investigación y Desarrollo
en Tecnología Farmacéutica
(UNITEFA), Córdoba, Argentina

Specialty section:

This article was submitted to
Molecular and Cellular Pathology,
a section of the journal
Frontiers in Cell and Developmental
Biology

Received: 14 January 2022

Accepted: 14 February 2022

Published: 01 March 2022

Citation:

Subirada PV, Vaglianti MV, Joray MB,
Paz MC, Barcelona PF and
Sánchez MC (2022) Rapamycin and
Resveratrol Modulate the Gliotic and
Pro-Angiogenic Response in Müller
Glial Cells Under Hypoxia.
Front. Cell Dev. Biol. 10:855178.
doi: 10.3389/fcell.2022.855178

¹Universidad Nacional de Córdoba, Facultad de Ciencias Químicas, Departamento de Bioquímica Clínica, Córdoba, Argentina, ²Consejo Nacional de Investigaciones Científicas y Técnicas (CONICET), Centro de Investigaciones en Bioquímica Clínica e Inmunología (CIBICI), Córdoba, Argentina, ³Universidad Católica de Córdoba, Facultad de Ciencias Químicas, Córdoba, Argentina, ⁴Consejo Nacional de Investigaciones Científicas y Técnicas (CONICET), Instituto de Investigaciones en Recursos Naturales y Sustentabilidad José Sánchez Labrador J. S., Córdoba, Argentina

Hypoxia and hypoxia-reoxygenation are frequently developed through the course of many retinal diseases of different etiologies. Müller glial cells (MGCs), together with microglia and astrocytes, participate firstly in response to the injury and later in the repair of tissue damage. New pharmacological strategies tend to modulate MGCs ability to induce angiogenesis and gliosis in order to accelerate the recovery stage. In this article, we investigated the variation in autophagy flux under hypoxia during 4 h, employing both gas culture chamber (1% O₂) and chemical (CoCl₂) hypoxia, and also in hypoxia-reoxygenation. Then, we delineated a strategy to induce autophagy with Rapamycin and Resveratrol and analysed the gliotic and pro-angiogenic response of MGCs under hypoxic conditions. Our results showed an increase in LC3B II and p62 protein levels after both hypoxic exposure respect to normoxia. Moreover, 1 h of reoxygenation after gas hypoxia upregulated LC3B II levels respect to hypoxia although a decreased cell survival was observed. Exposure to low oxygen levels increased the protein expression of the glial fibrillary acid protein (GFAP) in MGCs, whereas Vimentin levels remained constant. In our experimental conditions, Rapamycin but not Resveratrol decreased GFAP protein levels in hypoxia. Finally, supernatants of MGCs incubated in hypoxic conditions and in presence of the autophagy inducers inhibited endothelial cells (ECs) tubulogenesis. In agreement with these results, reduced expression of vascular endothelial growth factor (VEGF) mRNA was observed in MGCs with Rapamycin, whereas pigment epithelium-derived factor (PEDF) mRNA levels significantly increased in MGCs incubated with Resveratrol. In conclusion, this research provides evidence about the variation of autophagy flux under hypoxia and hypoxia-reoxygenation as a protective mechanism activated in response to the injury. In addition, beneficial effects were observed with Rapamycin treatment as it decreased the gliotic response and prevented the development of newly formed blood vessels.

Keywords: autophagy, hypoxia, angiogenesis, vascular endothelial growth factor, pigment epithelium-derived factor, gliosis

INTRODUCTION

As part of the Central Nervous System, the retina is highly dependent on nutrients and bioactive molecules, among them oxygen (Country, 2017). Extensive research has demonstrated that excessive or defective supply of oxygen is sufficient to trigger retinal damage or dysfunction (Caprara and Grimm, 2012). Retinopathy of prematurity (ROP) is a neonatal pathology that evidence this statement, as the events taking place in both the hyperoxic and the hypoxic phases are responsible for neuronal demise and glial activation (Ridano et al., 2017). In other retinal disorders as retinal vein occlusion, sickle cell anemia or diabetic retinopathy during the proliferative stage (PDR), hypoxia is solely detected.

Either constant or intermittent hypoxia is perceived as a threatening stimulus for retinal neurons. As a consequence, a fast response is settled by glial cells. Müller glial cells (MGCs), the most abundant macroglial cells of the retina, are known to collaborate in the immune response by secreting several cytokines, and to lead the vaso-proliferative response under hypoxia (Liu et al., 2014; Eastlake et al., 2016; Li et al., 2019). Many proteins participate in angiogenesis, including pro-angiogenic factors as the vascular endothelial growth factor (VEGF) and anti-angiogenic factors as pigment epithelium-derived factor (PEDF) (Eichler et al., 2004). Although these factors are secreted by many retinal cells, conditional VEGF KO mice revealed that the contribution of MGCs is indispensable for the vascular proliferation (Wang et al., 2010). Several signaling pathways can regulate VEGF synthesis or secretion. Therefore, a wide variety of compounds are able to modulate VEGF during pathological angiogenesis (Formica et al., 2021; Szymanska et al., 2021).

Another protective mechanism activated upon damage is autophagy. Autophagy is an intracellular catabolic process that ensure the degradation of misfolded proteins and altered organelles in the damaged tissue. Changes in autophagic flux can either induce cell survival or death. In this sense, treatments with different autophagy modulators proved to reduce cellular death or improve tissue function in disease (Kunchithapautham et al., 2011; Lin and Xu, 2019). On the other hand, autophagy inductors have demonstrated to exert pleiotropic effects in cells, including the secretion of trophic factors, affecting the fate of neighbor cells (Li et al., 2014; Zhou et al., 2018; Zwanzig et al., 2021). Two potent autophagy inductors are Rapamycin and Resveratrol. These compounds have attracted increasing attention in the research field because of their antioxidant and anti-angiogenic effects (Lee et al., 2015; Xin et al., 2017; Zhou et al., 2021). In ischemic retinopathies, it results interesting to evaluate if autophagy inductors under hypoxic conditions modulate the secretion of anti- or pro-angiogenic factors in MGCs and therefore vascular outgrowth.

Here, we initially investigated the variation in the autophagy flux under hypoxia and hypoxia-reoxygenation. Based on these results, we then delineated a strategy to induce autophagy with Rapamycin and Resveratrol and analysed the gliotic and pro-angiogenic response of MGCs under hypoxic conditions.

MATERIALS AND METHODS

Cell Line and Culture Reagents

A spontaneously immortalized human MGC line (MIO-M1), kindly provided by G. Astrid Limb (UCL Institute of Ophthalmology and Moorfields Eye Hospital, London, United Kingdom), was used. Cells were grown in Dulbecco's modified Eagle's medium (DMEM; Invitrogen, Buenos Aires, Argentina) containing 4500 mg/L glucose, sodium pyruvate) with 2 mM L-glutamine (GlutaMAX; Invitrogen), 10% vol/vol fetal bovine serum (FBS), and 50 U/mL penicillin/streptomycin (Invitrogen). Bovine aortic endothelial cells (BAECs) were grown in DMEM supplemented with 20% vol/vol FBS, and penicillin (100 U/mL)/streptomycin (100 U/mL) (Invitrogen). BAECs' media contained 0, 03 mg/ml of endothelial cell growth supplement from bovine pituitary (Sigma). Cell cultures were kept at 37°C in a 5% CO₂ humidified environment.

Hypoxic Assays

For gas hypoxia, cells were grown at 50–60% confluence in normal conditions and then transferred to a gas culture chamber (StemCell Technologies, Vancouver, Canada) supplied with 1% O₂, 94% N₂, and 5% CO₂. Control cells were kept in normoxia (21% O₂). For chemical hypoxia, cells were grown at 50–60% confluence in 10% FBS and then a solution of CoCl₂ (Cicarelli, Santa Fe, Argentina) diluted in PBS was added to the cell medium. Cell experiments were conducted at two different time points (4 and 24 h). To assess the autophagy flux, Chloroquine (CQ) diluted in PBS was added to result in a final concentration of 10 μM (24 h of exposure) or 50 μM (4 h of exposure). Some experiments included incubations with inductors (50 μM Rapamycin, 100 μM Resveratrol) of the autophagic flux, in presence or absence of CQ. All experiments were carried out in 10% FBS, as fasting constitutes an additional stimulus for autophagy.

For reoxygenation, hypoxic medium was replaced for standard medium and cells were incubated for 1 h at 37°C with 5% CO₂.

MTT Assay

To determine cell viability, the colorimetric MTT assay was performed. Briefly, 2,000 cells per well were seed in a 96-well plate and incubated under different experimental conditions (normoxia, hypoxia, CoCl₂, with or without Rapamycin or Resveratrol) for 24 h. Then, 10 μl of the yellow tetrazolium salt 3-(4, 5-dimethylthiazol-2-yl)-2, 5-diphenyltetrazolium bromide (MTT) (5 mg/ml) was added to culture medium. Cells were incubated with the MTT reagent for additional 3 h at 37°C. After that, cell medium was carefully removed and 100 μl of DMSO was added in order to solubilize the crystal violet. Finally, the optical density values were measured at a wavelength of 570 nm using a SpectraMax M5 plate reader (Molecular Devices, United States).

Western Blot Assay

Following treatment, cells were lysed with a solution of Triton X-100 1% in PBS, 1 mM PMSF and protease inhibitor cocktail

(Sigma Aldrich, St. Louis, MO). Lysates were cleared of insoluble material by centrifugation at 15,000 g for 10 min at 4°C. Protein concentration of MIO-M1 cell extracts were measured by a Bicinchoninic Acid Protein Assay Kit (Pierce BCA, Thermo Scientific, United States) according to the manufacturer's protocol and 20 µg of proteins were electrophoresed in 15% SDS-PAGE. After electrophoresis, proteins were transferred to nitrocellulose membranes (Amersham Hybond ECL; GE Healthcare Bio-Sciences AB, Uppsala, Sweden). To prevent nonspecific binding, membranes were blocked with 5% milk in TBS containing 0.1% Tween-20 (TBST) during 1 h at room temperature (RT). Then, blots were incubated with primary antibodies diluted in 1% BSA in TBST overnight at 4°C. The following antibodies were used: rabbit polyclonal anti-LC3 (1/1000; L7543, Sigma Aldrich), mouse monoclonal anti p62 (1/1000; ab56416, Abcam), rabbit polyclonal anti-GFAP (1/1000; Dako, Carpinteria, CA), mouse monoclonal anti-Vimentin (1/1000; M7020, Dako) and mouse monoclonal anti-β-actin (1/2000; ab8226, Abcam). Blots were incubated with IRDye 800 CW donkey anti-rabbit Ig, or IRDye 800 CW donkey anti-mouse IgG antibodies (1/15000 in TBS with 5% BSA) for 1 h, protected from light. After washing with TBST, membranes were visualized and quantified using the Odyssey Infrared Imaging System (LI-COR, Inc., Lincoln, NE, United States).

Immunofluorescence Assays and Confocal Microscopy

Briefly, cells were grown at 30% confluence on coverslips. For staining with the lysosome marker LysoTracker Red (Thermo Fisher Scientific) 1 µl/ml of the reagent was added to the cell medium in the final hour of the incubation time. After stimuli, coverslips were washed twice with precooled PBS and fixed in PBS containing 4% PFA/4% sucrose for 15 min at RT. Free aldehyde groups were blocked with 50 mM NH₄Cl in PBS during 20 min. The cells were then incubated in a blocking buffer (PBS containing 0.05% saponin/0.2% BSA) for 30 min. Antibodies were prepared in blocking buffer. Cells were then incubated overnight at 4°C with the following primary antibodies: rabbit polyclonal anti-LC3 (1/100; L7543, Sigma Aldrich), mouse monoclonal anti p62 (1/100; ab56416, Abcam). Then, cells were washed three times with PBS plus 1% BSA, and exposed to secondary antibodies diluted 1:800 for 45 min at RT. After a thorough rinse with PBS plus 1% BSA, cell nuclei were also counterstained with Hoechst 33258 (1:1000; Molecular Probes) for 7 min. Cells were washed with PBS and mounted on glass slides with Mowiol 4–88 (Calbiochem; Merck KGaA, Darmstadt, Germany). Fluorescent images were obtained with a confocal laser-scanning biological microscope (Olympus FluoView FV1200; Olympus Corp., New York, NY, United States). Finally, images were processed with ImageJ FIJI software (National Institutes of Health, Bethesda, MD, United States).

qRT-PCR

Total RNA was extracted from cultured cells using Trizol Reagent (Invitrogen) (Ridano et al., 2012). Briefly, 1 µg of total RNA was reverse-transcribed in a total volume of 20 µl using random primers (Invitrogen, Buenos Aires, Argentina) and 50 U of M-MLV reverse transcriptase (Promega Corp.). Then, cDNA was mixed with 1x SYBR

Green PCR Master Mix (Applied Biosystems) and forward and reverse primers: Beclin-1 forward: CCATGCAGGTGAGCTTCGT/Beclin-1 reverse: GAATCTGCGAGAGACACCATC; ATG5 forward: AAAGATGTGCTTCGAGATGTGT/ATG5 reverse: CACTTTGTCAGTACCAACGTCA. VEGF-A forward: CCGCAGACGTGATAAATGTTTCCT/VEGF-A reverse: CCGCTTGTCACATCTGCAAGTA; PEDF forward: GCTGAGTTACGAAGGCGAAGT/PEDF reverse: TTGATGGGT TTGCTGTGAT. qPCR were carried out on an Applied Biosystems 7500 Real-Time PCR System with Sequence Detection Software v1.4. The cycling conditions included a hot start at 95°C for 10 min, followed by 40 cycles at 95°C for 15 s and 60°C for 1 min. Specificity was verified by melting curve analysis. Results were normalized to β-actin (Forward: AAATCTGGCACCACACCTTC/Reverse: GGGGTGTGAAGGTCTCAAAA). Relative gene expression was calculated according to the ²-ΔΔCt method. Each sample was analyzed in triplicate. No amplification was observed in PCRs using as template water (data not shown).

Tube Formation Assay

The assay was performed according to Arnaoutova y Kleinman, (Arnaoutova and Kleinman, 2010). Briefly, BAEC (≈1.5 × 10⁴ cells) were placed on a 96 well half area plate previously coated with 30 µl of Matrigel. The plates were incubated for 18 h (37°C, 5% CO₂) in the presence of normoxic or hypoxic MIO-M1 supernatants containing vehicle or autophagy inductors. Sodium suramine 30 µM and Axitinib 10 µM were used as positive control of inhibition. Control samples with and without their respective vehicles were simultaneously run. The images were obtained with an Olympus CKX41 inverted microscope and analyzed with the software ImageJ. The tubular structures were quantified and the percentages of inhibition (I%) were calculated I% = [1-(Total tube length treatment/Total tube length control)] x 100.

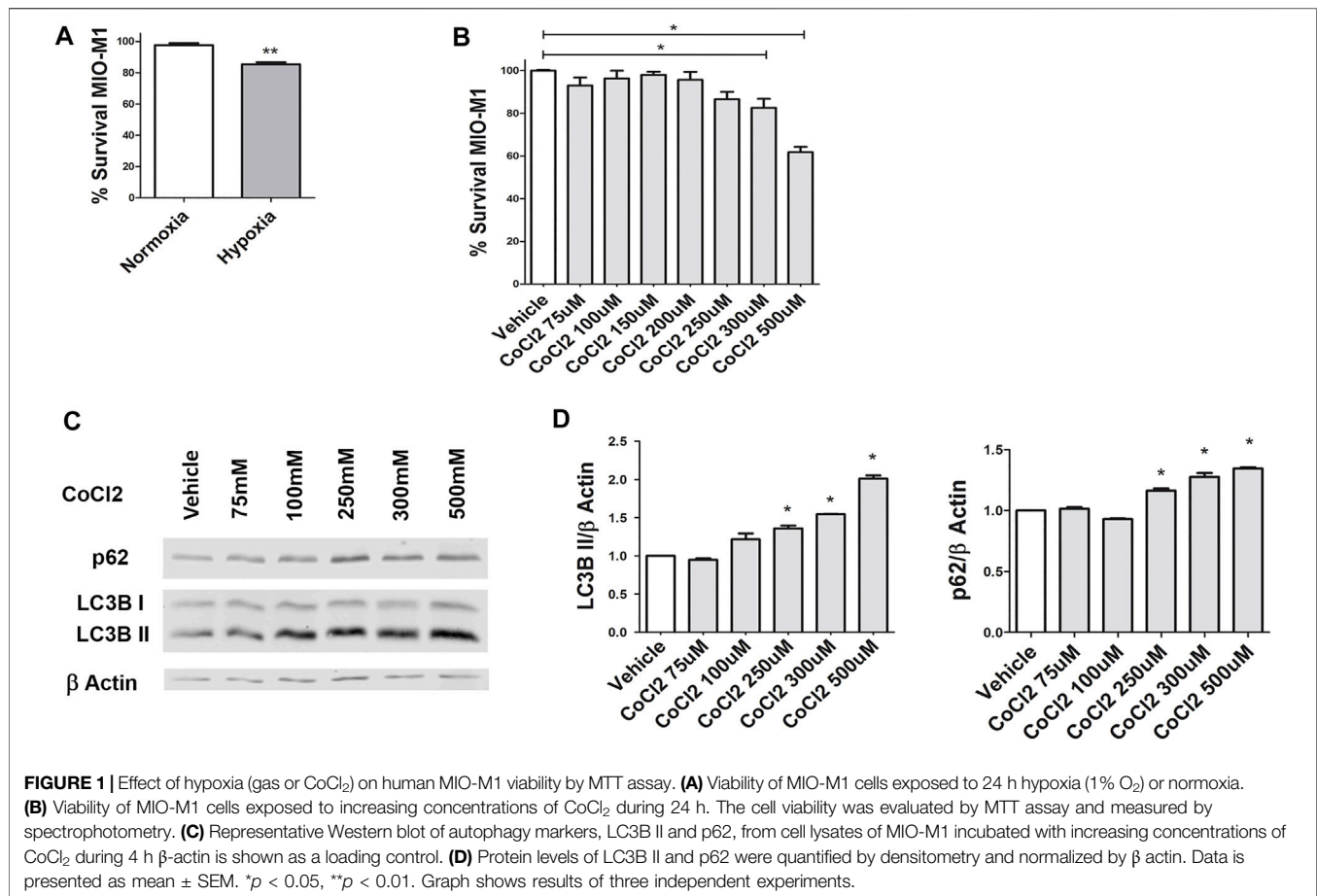
Statistical Analysis

Statistical analysis was performed using the GraphPad Prism 7.0 software. A p-value < 0.05 was considered statistically significant. Parametric or nonparametric tests were used according to variance homogeneity evaluated by F or Barlett's tests. Two-tailed unpaired t or Mann Whitney tests were used in analysis of two groups. One-way analysis of variance (ANOVA) followed by Dunnett's multiple comparison post-test or Kruskal-Wallis followed by Dunn's multiple comparison post-test were used to determine statistical significance among more than two different groups. Mean ± standard error (SEM) are shown in graphs analysed with parametric tests and median with interquartile range are shown when data were analysed with nonparametric test.

RESULTS

Autophagic Flux is Increased in MIO-M1 Cells Exposed to 4 h of Hypoxia

Previous studies conducted in MGCs exposed to hyperglycemia showed an altered autophagic flux given that autophagosomes could not reach the degradation step (Lopes de Faria et al., 2016).



However, in a hypoxic environment rat MGCs displayed an increase in LC3B II protein levels (Fung et al., 2016). Thereby, our first aim was to evaluate changes in the autophagic flux in human MGCs (MIO-M1), under hypoxia. Two experimental hypoxic models were used: the gas culture chamber (cells exposed to 1% O_2) and a chemical model (cells exposed to CoCl_2). Our experimental design included controls with and without Chloroquine (CQ) in order to assess the accumulation of the autophagosomes.

Although MGCs are very perceptive to environmental changes, they are considered the most resistant retinal cells to external injuries (Coughlin et al., 2017). In order to examine MIO-M1 survival under both hypoxic models, we carried out MTT assays at 24 h (Figure 1). MIO-M1 viability was reduced by 15% when exposed to 1% O_2 compared to normoxia ($p = 0.001$) (Figure 1A). For chemical hypoxia, we tested increasing concentrations of CoCl_2 . Viability of MIO-M1 cells exposed to CoCl_2 up to 250 μM did not change significantly respect to the control ($p = 0.1358$) (Figure 1B). Of note, no significant differences were observed in the MIO-M1 viability for shorter exposure periods (4 and 8 h, data not shown). Then, we studied changes in the expression of autophagic proteins in MIO-M1 cells exposed to CoCl_2 for 4 h by Western blot (Figure 1C). LC3B II (a structural protein of the autophagosomes) and p62 (an adaptor protein that is degraded with the autophagosome content) were

evaluated. The quantitative analyses of LC3B II and p62 bands evidenced a significant increase in the autophagic protein levels since a concentration of 250 μM respect to vehicle ($p = 0.027$ for LC3B II and $p = 0.031$ for p62). Therefore, we selected 250 μM CoCl_2 as a concentration for *in vitro* studies as it represents the minimum concentration that achieves two relevant requisites: it is not detrimental for cell viability and it is able to induce the autophagic flux.

Autophagy is a catabolic process rapidly activated in response to environmental stimuli that enables the cell adaptation to the new living conditions (Mizushima and Komatsu, 2011). Hence, we decided to evaluate if hypoxia modified the autophagic flux in human MGCs exposed to short periods. For this purpose, the MIO-M1 cells were exposed to hypoxia or normoxia during 4 h, in presence of CQ or vehicle in the above indicated conditions. Simultaneously, a comparative study was performed by incubating MIO-M1 cells with CoCl_2 250 μM , including controls with and without CQ (Figure 2). By Western blot assay we observed no significant changes in LC3B II and p62 protein expression levels in gas hypoxia or CoCl_2 respect to normoxia in absence of CQ. However, in samples treated with CQ a significant increase in LC3B II protein levels was observed under both hypoxic treatments ($p = 0.0447$ for 1% O_2 and $p = 0.0021$ for CoCl_2) respect to normoxia.

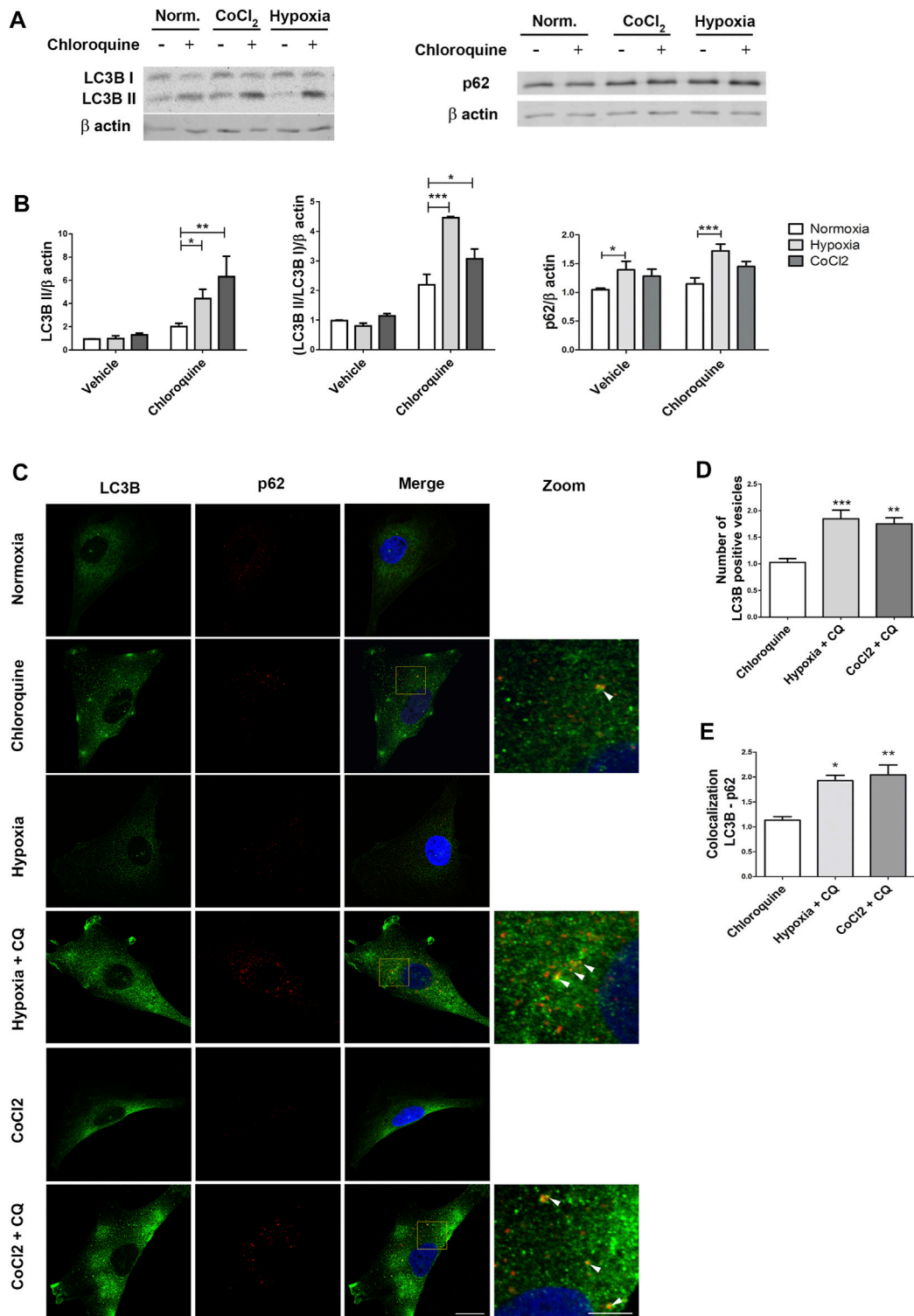


FIGURE 2 | Hypoxia increases LC3B II and p62 protein levels in MIO-M1. **(A)** Representative Western blot of autophagy markers, LC3B II and p62, from cellular lysates of MIO-M1 incubated in hypoxic conditions: gas (1% O₂) or chemical hypoxia (250 mM CoCl₂) during 4 h. **(B)** Protein levels of LC3B II and p62 were quantified by densitometry and normalized to β actin. Graph shows results of three independent experiments. **(C)** Representative immunofluorescence analysis of LC3B (green) and p62 (red) in MIO-M1 cells incubated in hypoxic conditions: gas (1% O₂) or CoCl₂ (250 mM) during 4 h. Cell nuclei were counterstained with Hoechst 33258 (blue). Images were taken with oil 60X objective in the best confocal resolution condition. **(D)** Quantification of LC3B puncta per cell with ImageJ analyze particles software. Values were normalized to normoxia + chloroquine. **(E)** Quantification of LC3B/p62 colocalization with ImageJ JACoP software. Pearson values were compared statistically. Values were normalized to normoxia + chloroquine. Statistical t test was performed. White arrows in the images show mayor colocalization areas. Data is presented as mean ± SEM. **p* < 0.05, ***p* < 0.01, ****p* < 0.001. Graph shows results of three independent experiments.

Under 1% O₂, MIO-M1 cells incubated with CQ showed a significant increase in p62 protein levels ($p = 0.0006$) (Figures 2A,B) respect to normoxia-CQ. Although we observed a non-significant increase in the expression of p62 in presence of CoCl₂ 250 μM ($p = 0.3959$), incubation with CQ showed a significant accumulation of LC3B II in MIO-M1 cells respect to vehicle, suggesting that the autophagic vesicles follow the degradation pathway properly.

Correlatively, immunofluorescence assays with classic markers of autophagy showed an increased number of LC3B puncta per cell in MIO-M1 exposed to gas hypoxia ($p < 0.001$) and CoCl₂ ($p = 0.005$), respect to normoxia (Figures 2C,D). In line with these results, a higher colocalization of LC3B and p62 was determined in both hypoxic conditions respect to normoxia ($p = 0.018$ for 1% O₂ and $p = 0.0069$ for CoCl₂) (Figure 2E).

Autophagic Flux Returns to Normoxic Levels After 24 h of Hypoxia in MIO-M1 Cells

Cell response to an injurious stimulus can vary depending on its duration. Therefore, we decided to evaluate MGCs behaviour under prolonged exposure to hypoxia (24 h) by analysing changes in their autophagic flux. Experimental conditions were similar to those in shorter hypoxic stimuli. By Western blot assays, similar protein expression levels of LC3B II and p62 were observed in MIO-M1 cells under gas hypoxia and normoxia when incubated with CQ ($p > 0.9999$ for LC3BII and $p = 0.2821$ for p62) (Supplementary Figures S1A,B). Then, we quantified mRNA levels of Beclin-1 and ATG5. Results showed a not statistically significant decrease in Beclin-1 and ATG-5 transcript levels in MIO-M1 cells under 1% O₂ ($p = 0.1248$ for Beclin-1 and $p = 0.0753$ for ATG5) (Supplementary Figure S1C). In contrast, an increase in autophagy protein levels was observed in cells incubated with CoCl₂ for 24 h in presence of CQ ($p = 0.0011$ for LC3BII and $p < 0.0001$ for p62) (Supplementary Figures S1A,B). In spite of this result, mRNA levels of Beclin-1 and ATG5 were not modified ($p = 0.7368$ for Beclin-1 and $p = 0.3638$ for ATG5), suggesting a slight activation of the autophagic flux (Supplementary Figure S1C). Confocal images of MIO-M1 cells exposed to hypoxia (1% O₂) and normoxia revealed similar number of LC3B puncta per cell ($p = 0.3081$) and colocalization of LC3B and p62 ($p = 0.2975$) (Supplementary Figures S1D–F). On the other hand, CoCl₂ induced an increase in the number of vesicles decorated with LC3B ($p = 0.0373$) and a slight rise in the colocalization of LC3B and p62 respect to control ($p = 0.0024$) (Supplementary Figures S2A–C). These results demonstrate a higher number of autophagosomes when MIO-M1 cells were exposed to CoCl₂ for 24 h respect to control. The late stage of the autophagy pathway involves the degradation of the autophagosome content and its inner membrane by fusion with lysosomes. In order to evidence the fusion of autophagosomes with lysosomes, immunofluorescence assays were performed with LC3B and LysoTracker, an acidic compartment and late endosomes marker. The colocalization analysis evidenced no difference in the overlap of the proteins when MIO-M1 cells were incubated with vehicle or CoCl₂ during 24 h ($p = 0.9738$) (Supplementary Figures S2D,E). Moreover, we also evaluated

the lysosomal membrane integrity by immunostaining with Galectin-1 (Gal-1). In our experiments, Gal-1 staining showed a homogeneous cytoplasmic distribution in MIO-M1 cells in both hypoxic models, suggesting that lysosomal structure was preserved after 24 h of exposure (Supplementary Figure S2F).

Autophagic Flux is Increased in MIO-M1 Cells After Reoxygenation

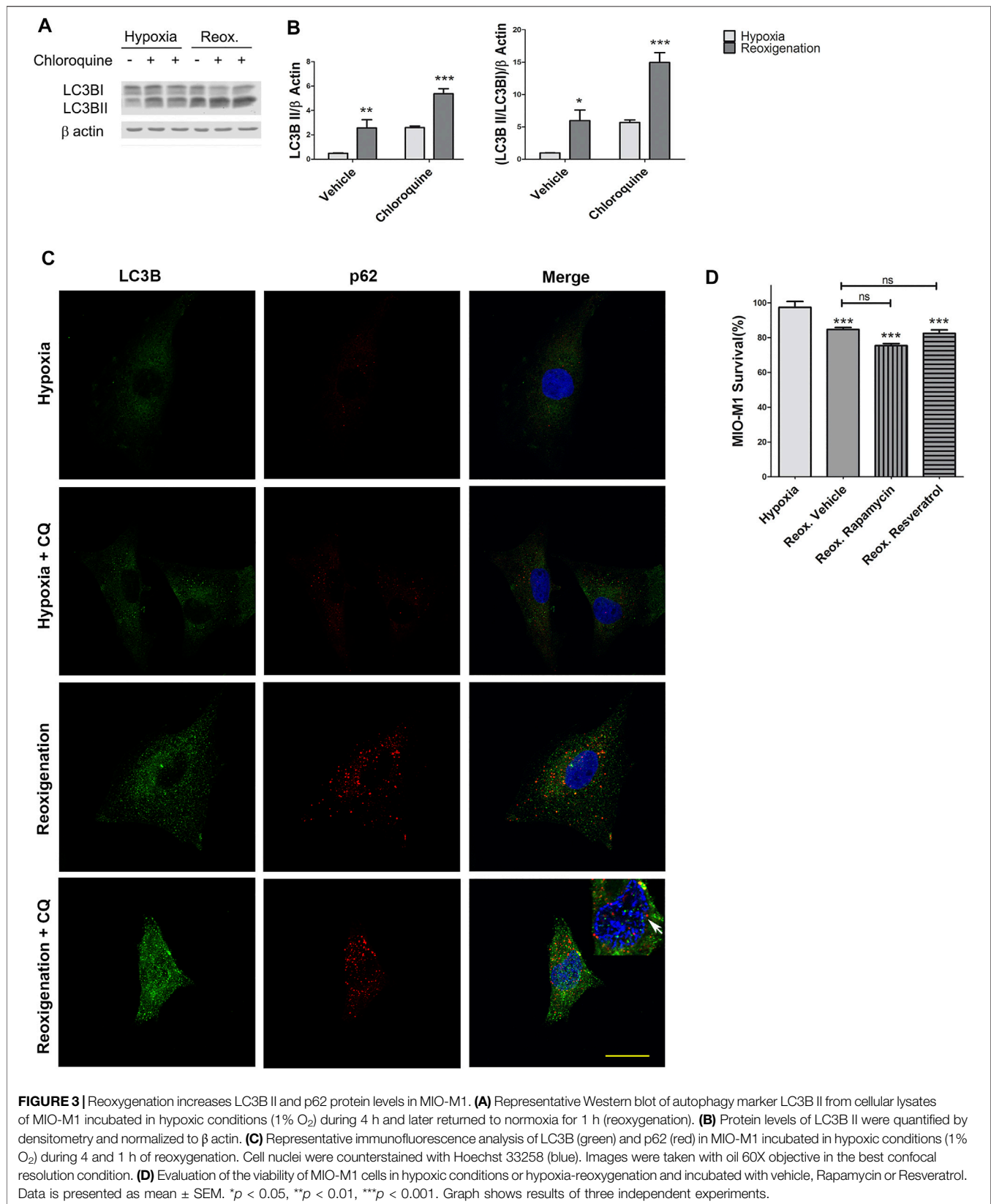
Clinical studies provided evidence about the variation of oxygen levels in neuronal tissues in patients with PDR (Daulatzai, 2017). Hence, we next evaluated the autophagic flux in MIO-M1 cells exposed to 4 h hypoxia followed by 1 h of reoxygenation. Quantitative analysis of Western blot assays revealed a significant increase in LC3B II ($p < 0.001$) in reoxygenated MIO-M1 cells compared to the hypoxic ones, in conditions with CQ (Figures 3A,B). In line with this results an increase in vesicles decorated by LC3B were observed in reoxygenated MIO-M1 cells in presence of CQ (Figure 3C), suggesting an increase in the number of autophagosomes when returned to normoxia after the hypoxic period. To determine the role of autophagy in reoxygenation, we assessed MIO-M1 survival by MTT assay (Figure 3D). The cell viability of the reoxygenated MIO-M1 cells was significantly lower than in hypoxic condition ($p = 0.0009$). In addition, inductors of the autophagic flux were unable to restore MIO-M1 survival ($p = 0.305$ for Reoxygenation + Rapamycin; $p = 0.9999$ for Reoxygenation + Resveratrol). Notably, the blockade of the flux with CQ induced cytoplasmic retraction and nuclear condensation in MIO-M1 cells under reoxygenation (Figure 3C, white arrow).

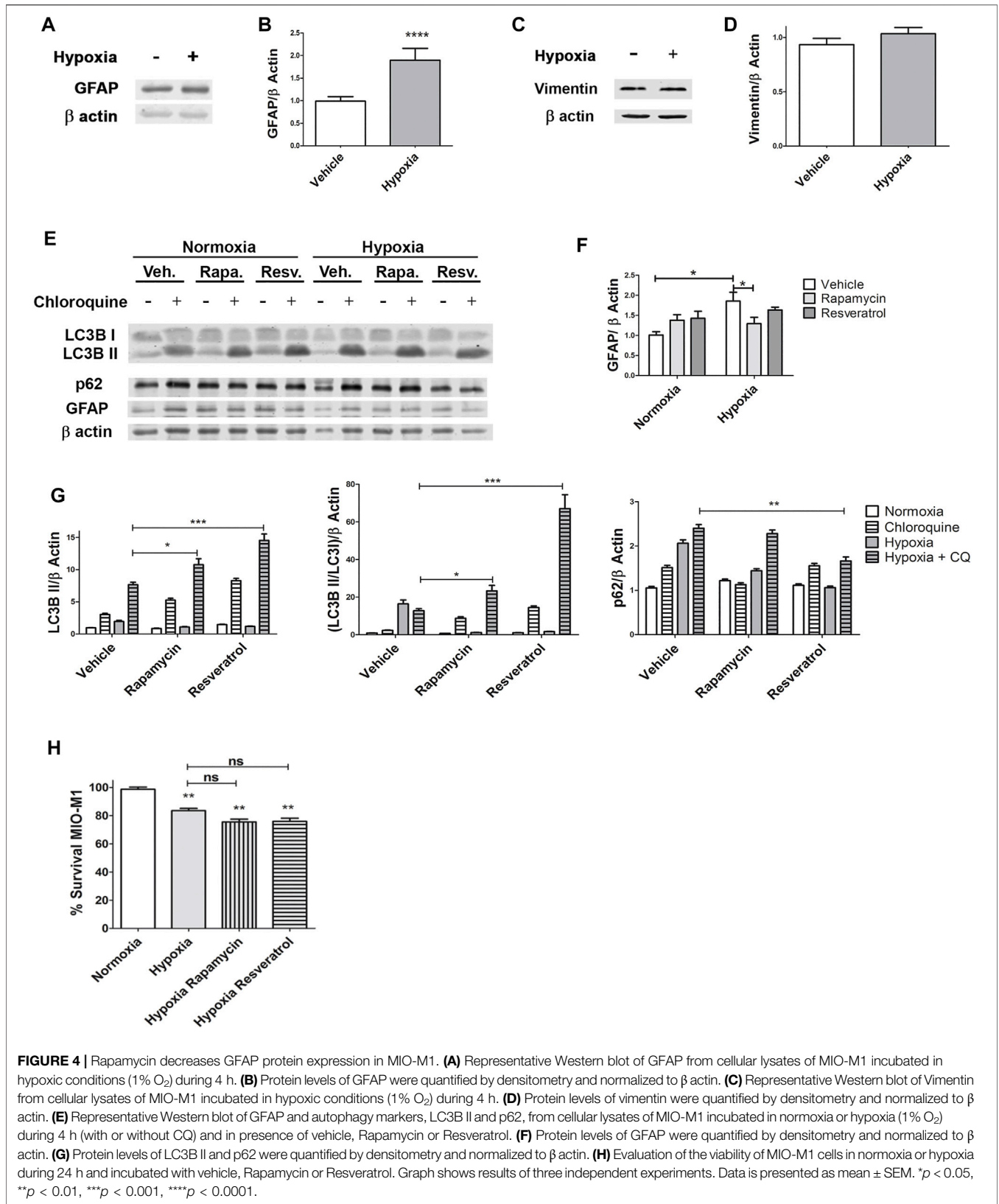
MIO-M1 Cells Gliosis is Decreased by Autophagy Inductors

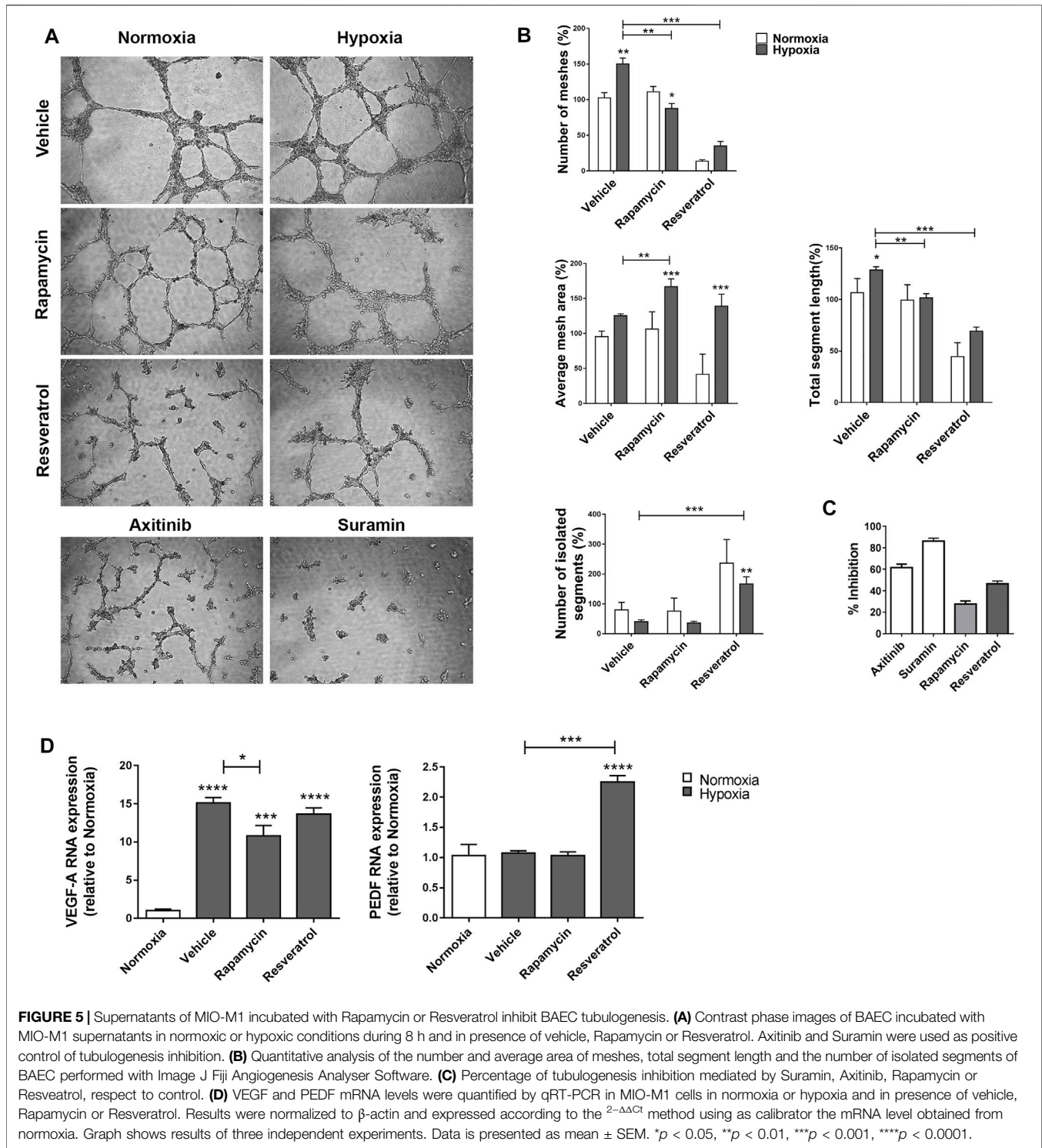
In response to an injury or stressor, MGCs trigger protective mechanisms in order to preserve retinal structure and functionality, a process called reactive gliosis (Subirada et al., 2018). We have previously demonstrated in a mouse model of Oxygen-induced retinopathy (OIR) that MGCs become reactive after the hyperoxic phase and modified the expression of stress and detoxifying proteins from postnatal days 12 to 26 in OIR mice (Ridano et al., 2017). Then, our next aim was to analyse changes in the expression levels of GFAP after hypoxic exposure. This set of experiments was performed with gas hypoxia, at the time where a main response to hypoxia was detected (4 h).

After 4 h of hypoxia, MIO-M1 cells showed an increase in protein levels of GFAP ($p < 0.0001$) in accordance with the activation of glial cells (Figures 4A,B), although no differences in Vimentin expression was detected ($p = 0.1012$) by Western blot assays (Figures 4C,D).

We have previously demonstrated in the OIR mouse model, a decrease in the GFAP protein levels after a single intraocular injection of Rapamycin at postnatal day 26 OIR (Subirada et al., 2019). Therefore, we aimed to determine if inductors of the autophagic flux prevented the increase of GFAP expression under hypoxic conditions. For this purpose, MIO-M1 cells were incubated in normoxia or hypoxia (1% O₂) and in







presence of Rapamycin or Resveratrol for 4 h. Western blot assays showed a substantial decrease in GFAP protein expression levels by Rapamycin in MIO-M1 cells exposed to 1% O₂ ($p = 0.0438$). A trend to diminish GFAP protein levels was observed in hypoxia/Resveratrol, however, this decrease was not statistically significant

($p = 0.6558$) (Figures 4E,F). We confirmed the induction of the autophagic flux in this experiment by analysis of LC3B II and p62 protein levels (Figures 4E,G). Lastly, we evaluated if autophagy inductors could prevent cell death after 24 h of hypoxia, the only experimental time point where decreased viability was observed

(**Figure 1A**). The MTT assay showed that MIO-M1 cells incubated with either of the inductors exhibited similar cell survival respect to hypoxia vehicle ($p = 0.0834$ for hypoxia + Rapamycin; $p = 0.1337$ for hypoxia + Resveratrol) (**Figure 4H**).

MIO-M1 Cells Modulate Angiogenesis in Presence of Autophagy Inductors

It is known that MGCs maintain the vascular structure through a balance between synthesis and secretion of pro- and anti-angiogenic factors. Thus, our next goal was to evaluate MGCs ability to induce tubulogenesis of endothelial cells (ECs) under hypoxia and how the inductors of the autophagy modified this response. For this purpose, we incubated MIO-M1 cells under normoxia or hypoxia (1% O₂) with an inductor of the autophagic flux or vehicle, and obtained their supernatants. Then, tubulogenesis assays were performed on Matrigel by incubating ECs with the supernatants of MIO-M1 cells during 24 h (**Figure 5A**). Suramin and Axitinib were used as negative controls of tubulogenesis. Quantitative analysis of the tubular network formed by ECs showed that hypoxic MIO-M1 supernatants increased the formation of vascular tubules respect to normoxic supernatants. We observed an increase in the mesh number (polygonal vascular structures) and the total segment length of vessel tubules in ECs incubated with hypoxic supernatants (**Figures 5A,B**). Then we compared ECs tubulogenesis incubated with supernatants containing vehicle respect to those containing an autophagy inductor. MIO-M1 supernatants exposed to hypoxia and in presence of Rapamycin decreased the mesh number, increased the average mesh area and decreased the total segment length respect to hypoxic + vehicle supernatant. Those changes were not observed between vehicle and Rapamycin in normoxic supernatants. On the other hand, Resveratrol modified all the quantified parameters, showing an evident decrease in the tubule formation respect to vehicle. Resveratrol had a similar effect when ECs were incubated with both normoxic and hypoxic MIO-M1 supernatants. In line with these results, both treatments in hypoxic supernatants showed a significant increase in the percentage of tubulogenesis inhibition respect to hypoxic-vehicle supernatant (**Figure 5C**). Finally, we examined if autophagy inductors had a direct effect over ECs. For that purpose, we incubated ECs with Rapamycin and Resveratrol for 24 h. We observed no variations in the formation of polygonal structures when ECs were incubated with either autophagy inductor respect to vehicle (**Supplementary Figure S3**).

It has been demonstrated that under hypoxic conditions MGCs are one of the cells responsible for the increase of VEGF retinal levels, the main pro-angiogenic factor involved in angiogenesis (Wang et al., 2010). To restrict the vascular growth, MGCs secrete PEDF, which counterbalance pro-angiogenic factors (Yang et al., 2012). In order to determine if trophic factors levels were modified by the autophagy inductors, we further quantified the transcript levels of VEGF and PEDF in hypoxic MIO-M1 cells (**Figure 5D**). Quantitative RT-PCR analysis showed an increase in VEGF mRNA levels in hypoxia respect to normoxia. Moreover, Rapamycin induced a significant decrease of VEGF mRNA respect to hypoxia vehicle ($p = 0.0334$).

VEGF transcript was not modified in MIO-M1 incubated in hypoxia + Resveratrol. By contrast, PEDF mRNA was only increased in hypoxic MIO-M1 cells treated with Resveratrol ($p = 0.0003$). In summary, the results indicate that Rapamycin and Resveratrol prevents tubule formation by modulating different proteins involved in angiogenesis.

DISCUSSION

MGCs provide neuronal support and communicate with other cells in order to maintain retinal homeostasis. Their roles in health and disease are indispensable for neuronal survival, however, they also undergo changes and eventually die after an injury. Autophagy is a catabolic pathway that can be up- or down-regulated in ischemic retinopathies. The increase in the autophagic flux has been linked to cell survival as it removes ROS or damaged organelles and proteins (Kroemer et al., 2010). However, under specific circumstances, excessive activation can also lead to cell death. With a proper pharmacological therapy, autophagy modulators have prevented neurodegeneration in several animal models (Lin and Xu, 2019). Autophagy inductors are a group of compounds that are able to increase autophagy flux. Their effects are exerted by the regulation of different signaling pathways that modulate autophagic flux but also by inducing other cellular events (Li et al., 2014; Zhou et al., 2018).

In a previous study we showed that induction and inhibition of the autophagic flux had a direct impact on vascular and glial events in the experimental OIR mouse model (Subirada et al., 2019). Here, we evaluated the ability of two autophagy inductors to modulate MGC functions under hypoxia.

Initially, we evaluated variations in the autophagic flux of human MGCs under two hypoxic models (gas and chemical during 4 h). In both models, we observed augmented LC3B II protein levels respect to normoxia in presence of CQ, suggesting an increase in the autophagic flux. The accumulation of autophagosomes in presence of CQ respect to their corresponding vehicle controls demonstrate that the autophagic vesicles can reach the final stage of the degradation pathway. Quantitatively, the increase in LC3B II protein levels in MIO-M1 cells was higher under CoCl₂ than under gas hypoxia, indicating that the nature of the stimulus influences the intensity of the response. The increase in the number of LC3B vesicles and colocalization of LC3B and p62 reinforced these results as a major number of autophagosomes was observed in MIO-M1 cytoplasm under chemical and gas hypoxia. Similar results were obtained when incubating MIO-M1 cells under gas hypoxia. Although this work did not focus in the signalling pathways that activate autophagy under hypoxia, experiments performed with CoCl₂ constitute a reflex of the activation of the flux via HIF-1 α (Yuan et al., 2003). Respect to gas hypoxia, it is possible that other signalling pathways may also be activated (Li et al., 2015).

Autophagy is a catabolic mechanism by which altered proteins, organelles and others are recycled to amino acids in different stressful conditions, contributing to the reestablishment of the homeostasis (Klionsky et al., 2021). Thereby, it would be

predictable that the autophagic flux have a relevant role during initial stages of the stimulus, until the cell reach a stable metabolic state. Prolonged exposition frequently show a different autophagy flux (Zhang et al., 2020). By Western blot and immunofluorescence assays we demonstrated that autophagic flux returned to normoxic levels when incubated in 1% O₂ during 24 h. This result indicates that the activation of the flux is transient and takes place immediately after the exposition to hypoxic environment. Conversely, LC3B II and p62 protein levels remained elevated after a 24 h stimulus with CoCl₂. The increase in the ratio of LC3B II to LC3B I evidenced that the autophagic flux is still activated. At this final time point, a similar colocalization between LC3B and Lysotracker was observed in normoxic and hypoxic conditions, demonstrating that the fusion of autophagosomes and lysosomes is not altered by CoCl₂. On the other hand, a Gal-1 dotted pattern could be indicative of permeability and subsequent lysosomal dysfunction. No changes in Gal-1 staining pattern were detected under both hypoxic conditions respect to normoxia. All conditions exhibited a homogeneous cytoplasmic distribution of Gal-1, indicating that lysosomes are not permeable.

In this work, we also explored the variation in the autophagic flux after reoxygenation. Insulin resistance and metabolic derangement have been linked to sleep apnea and other sleeping disorders observed in diabetics, which can further induce nocturnal events of hypoxia and reoxygenation in the retina (Shiba et al., 2010; Thomas et al., 2017). As assessed by Western blot and confocal images, there is an increase in autophagosomes in MIO-M1 cells when reoxygenated respect to hypoxia. Moreover, the accumulation of LC3B II in hypoxia and reoxygenation with CQ respect to vehicle proved that there is no alteration in the degradation pathway in both experimental conditions. The restoration of oxygen levels to normoxia reduced the survival of MIO-M1 cells, probably due to the fast activation of the respiratory chain in presence of O₂ and subsequent production of reactive oxygen species. In this sense, the activation of autophagy could represent a protective response to oxidative stress damage. Unfortunately, autophagy results insufficient to preserve the cell survival, as observed by the addition of Rapamycin and Resveratrol. This poorly studied effect of oxygen levels variation at night would partly explain the neurodegeneration observed in the retina of PDR diabetic patients even after anti-angiogenic treatment.

The gliotic response triggered after an injury provides protection to all retinal cells. Key features in the gliotic response are the biochemical and morphological changes experienced by MGCs, which include the up-regulation of intermediate filaments and detoxification enzymes (Graca et al., 2018). In our cellular system, incubations at low oxygen levels for 4 h increased GFAP protein expression, a glial stress marker. Other filamentous protein, Vimentin, showed less sensibility to the hypoxic exposure, as its protein levels remained constant respect to normoxia. It has been shown that Rapamycin treatment decreased astroglial reactivity in several neurological pathologies (Siman et al., 2015; Liu et al., 2021). In our hypoxic MIO-M1 culture, we observed decreased GFAP expression after Rapamycin treatment, whereas

Resveratrol showed a non-significant reduction in this protein levels. We consider that the underlying mechanisms to this event could be different between both inductors, and even independent of the modulation of the autophagic flux. Overall, the ability of Rapamycin to prevent gliosis constitute a potential pharmacological strategy to cope with persistent gliosis, a relevant aspect of chronic ischemic retinopathies that is not improved with anti-VEGF treatment (Ridano et al., 2017). Unfortunately, at the concentrations evaluated, Rapamycin and Resveratrol were not able to mitigate cell death. Because the similar cell viability was detected in presence and absence of the inductors, we can conclude that autophagy is not the cell death mechanism involved in hypoxic cell death, but its activation is not sufficient to prevent MGCs death.

Finally, we examined another MGC function under hypoxia: its participation in vascular proliferation. A reduced formation of tubular structures was observed when ECs were incubated with MIO-M1 supernatants exposed to hypoxia and in presence of Rapamycin. The observation that normoxic supernatants with Rapamycin were not able to decrease tubulogenesis, demonstrates that Rapamycin anti-proliferative effect is exclusively exerted under hypoxia. The balance towards the anti-proliferative effect can be shifted by increasing the synthesis of anti-angiogenic proteins (as PEDF) or by decreasing the synthesis of the pro-angiogenic proteins (mainly VEGF) (Yafai et al., 2007). Accordingly, Rapamycin reduced VEGF mRNA as it was previously described (Liu et al., 2015; Kida et al., 2021). Instead, Resveratrol strongly inhibited ECs tubulogenesis in both hypoxic and normoxic MIO-M1 supernatants. In this regard, some studies have previously described the ability of Resveratrol to increase PEDF synthesis (Hua et al., 2011; Ishida et al., 2017). As expected, PEDF levels were increased in hypoxic conditions after Resveratrol treatment, suggesting an anti-angiogenic cell response. At the concentrations employed in this work, we did not observe a variation in the formation of tubular structures when the inductors were incubated directly with ECs. This result demonstrates that the antiangiogenic effects observed are mediated by MIO-M1 response.

In this research, we evaluated MGCs autophagy flux in two experimental hypoxic models, confirming the activation of an early autophagic response. At the same time, MGCs established a gliotic response and participated in vaso-proliferative events. Inductors of the autophagy flux partially reverted these responses, considering Rapamycin as the compound that more beneficial effects produced (**Supplementary Table S1**). Its ability to decrease persistent gliosis and reduce VEGF synthesis shows that Rapamycin modulates vascular and non-vascular alterations through direct effect on MGCs, two relevant aspects of ischemic retinopathies. Our results provide a general overview of the multiple benefits of MGCs modulation with autophagy inductors.

DATA AVAILABILITY STATEMENT

The original contributions presented in the study are included in the article/**Supplementary Material**, further inquiries can be directed to the corresponding author.

AUTHOR CONTRIBUTIONS

PS and MS conceived and designed experiments. PS, MV, and MJ carried out experiments. PS, MV, MJ, and MS interpreted data. PB and MP contributed new reagents/analytic tools, analysed and discussed data. PS and MS wrote and reviewed critically the manuscript. All authors had final approval of the submitted and published versions.

FUNDING

This work was funded by grants from Secretaría de Ciencia y Tecnología, Universidad Nacional de Córdoba (SECyT-UNC) Consolider 2018–2021, Fondo para la Investigación Científica y Tecnológica (FONCyT), Proyecto de Investigación en Ciencia y Tecnología (PICT) 2015 N° 1314 and PIP (CONICET) 2021–2023 (All to MS).

REFERENCES

- Arnaoutova, I., and Kleinman, H. K. (2010). *In Vitro* angiogenesis: Endothelial Cell Tube Formation on Gelled Basement Membrane Extract. *Nat. Protoc.* 5 (4), 628–635. doi:10.1038/nprot.2010.6
- Caprara, C., and Grimm, C. (2012). From Oxygen to Erythropoietin: Relevance of Hypoxia for Retinal Development, Health and Disease. *Prog. Retin. Eye Res.* 31 (1), 89–119. doi:10.1016/j.preteyeres.2011.11.003
- Coughlin, B. A., Feenstra, D. J., and Mohr, S. (2017). Müller Cells and Diabetic Retinopathy. *Vis. Res.* 139, 93–100. doi:10.1016/j.visres.2017.03.013
- Country, M. W. (2017). Retinal Metabolism: A Comparative Look at Energetics in the Retina. *Brain Res.* 1672, 50–57. doi:10.1016/j.brainres.2017.07.025
- Daulatzai, M. A. (2017). Cerebral Hypoperfusion and Glucose Hypometabolism: Key Pathophysiological Modulators Promote Neurodegeneration, Cognitive Impairment, and Alzheimer's Disease. *J. Neurosci. Res.* 95 (4), 943–972. doi:10.1002/jnr.23777
- Eastlake, K., Banerjee, P. J., Angbohang, A., Charteris, D. G., Khaw, P. T., and Limb, G. A. (2016). Müller Glia as an Important Source of Cytokines and Inflammatory Factors Present in the Gliotic Retina during Proliferative Vitreoretinopathy. *Glia* 64 (4), 495–506. doi:10.1002/glia.22942
- Eichler, W., Yafai, Y., Wiedemann, P., and Reichenbach, A. (2004). Angiogenesis-related Factors Derived from Retinal Glial (Müller) Cells in Hypoxia. *Neuroreport* 15 (10), 1633–1637. doi:10.1097/01.wnr.0000133071.00786.a4
- Formica, M. L., Awde Alfonso, H. G., and Palma, S. D. (2021). Biological Drug Therapy for Ocular Angiogenesis: Anti-VEGF Agents and Novel Strategies Based on Nanotechnology. *Pharmacol. Res. Perspect.* 9 (2), e00723. doi:10.1002/prp2.723
- Fung, F. K., Law, B. Y., and Lo, A. C. (2016). Lutein Attenuates Both Apoptosis and Autophagy upon Cobalt (II) Chloride-Induced Hypoxia in Rat Müller Cells. *PLoS one* 11 (12), e0167828. doi:10.1371/journal.pone.0167828
- Graca, A. B., Hippert, C., and Pearson, R. A. (2018). Müller Glia Reactivity and Development of Gliosis in Response to Pathological Conditions. *Adv. Exp. Med. Biol.* 1074, 303–308. doi:10.1007/978-3-319-75402-4_37
- Hua, J., Guerin, K. I., Chen, J., Michán, S., Stahl, A., Krah, N. M., et al. (2011). Resveratrol Inhibits Pathologic Retinal Neovascularization in Vldlr^{-/-} Mice. *Invest. Ophthalmol. Vis. Sci.* 52 (5), 2809–2816. doi:10.1167/iovs.10-6496
- Ishida, T., Yoshida, T., Shinohara, K., Cao, K., Nakahama, K. I., Morita, I., et al. (2017). Potential Role of Sirtuin 1 in Müller Glial Cells in Mice Choroidal Neovascularization. *PLoS one* 12 (9), e0183775. doi:10.1371/journal.pone.0183775
- Kida, T., Oku, H., Osuka, S., Horie, T., and Ikeda, T. (2021). Hyperglycemia-induced VEGF and ROS Production in Retinal Cells Is Inhibited by the mTOR Inhibitor, Rapamycin. *Scientific Rep.* 11 (1), 1885. doi:10.1038/s41598-021-81482-3

ACKNOWLEDGMENTS

We thank Carlos Mas, María Pilar Crespo and Cecilia Sampedro of CEMINCO (Centro de Micro y Nanoscopia Córdoba, 588 CONICET-UNC, Córdoba, Argentina) for assistance in confocal microscopy, Laura Gatica for histological assistance, Gabriela Furlán for culture cell facility support and Luciana Reyna for Molecular assistance. PS is postdoctoral fellow of CONICET, MV is doctoral fellow of CONICET, MJ, MP, PB, and MS are members of the Research Career of CONICET.

SUPPLEMENTARY MATERIAL

The Supplementary Material for this article can be found online at: <https://www.frontiersin.org/articles/10.3389/fcell.2022.855178/full#supplementary-material>

- Klionsky, D. J., Abdel-Aziz, A. K., Abdelfatah, S., Abdellatif, M., Abdoli, A., Abel, S., et al. (2021). Guidelines for the Use and Interpretation of Assays for Monitoring Autophagy (4th Edition). *Autophagy* 17 (1), 1–382. doi:10.1080/15548627.2020.1797280
- Kroemer, G., Mariño, G., and Levine, B. (2010). Autophagy and the Integrated Stress Response. *Mol. Cell.* 40 (2), 280–293. doi:10.1016/j.molcel.2010.09.023
- Kunchithapautham, K., Coughlin, B., Lemasters, J. J., and Rohrer, B. (2011). Differential Effects of Rapamycin on Rods and Cones during Light-Induced Stress in Albino Mice. *Invest. Ophthalmol. Vis. Sci.* 52 (6), 2967–2975. doi:10.1167/iovs.10-6278
- Lee, C. S., Choi, E. Y., Lee, S. C., Koh, H. J., Lee, J. H., and Chung, J. H. (2015). Resveratrol Inhibits Hypoxia-Induced Vascular Endothelial Growth Factor Expression and Pathological Neovascularization. *Yonsei Med. J.* 56 (6), 1678–1685. doi:10.3349/ymj.2015.56.6.1678
- Li, J., Kim, S. G., and Blenis, J. (2014). Rapamycin: One Drug, many Effects. *Cel Metab.* 19 (3), 373–379. doi:10.1016/j.cmet.2014.01.001
- Li, M., Tan, J., Miao, Y., Lei, P., and Zhang, Q. (2015). The Dual Role of Autophagy under Hypoxia-Involvement of Interaction between Autophagy and Apoptosis. *Apoptosis* 20 (6), 769–777. doi:10.1007/s10495-015-1110-8
- Li, X., Liu, J., Hoh, J., and Liu, J. (2019). Müller Cells in Pathological Retinal Angiogenesis. *Transl. Res.* 207, 96–106. doi:10.1016/j.trsl.2018.12.006
- Lin, W., and Xu, G. (2019). Autophagy: A Role in the Apoptosis, Survival, Inflammation, and Development of the Retina. *Ophthalmic Res.* 61 (2), 65–72. doi:10.1159/000487486
- Liu, J., Li, R., Huang, Z., Lin, J., Ji, W., Huang, Z., et al. (2021). Rapamycin Preserves Neural Tissue, Promotes Schwann Cell Myelination and Reduces Glial Scar Formation after Hemi-Contusion Spinal Cord Injury in Mice. *Front. Mol. Neurosci.* 13, 574041. doi:10.3389/fnmol.2020.574041
- Liu, N. N., Zhao, N., and Cai, N. (2015). Suppression of the Proliferation of Hypoxia-Induced Retinal Pigment Epithelial Cell by Rapamycin through the mTOR/HIF-1 α /VEGF/Signaling. *IUBMB life* 67 (6), 446–452. doi:10.1002/iub.1382
- Liu, X., Ye, F., Xiong, H., Hu, D., Limb, G. A., Xie, T., et al. (2014). IL-1 β Upregulates IL-8 Production in Human Müller Cells through Activation of the P38 MAPK and ERK1/2 Signaling Pathways. *Inflammation* 37 (5), 1486–1495. doi:10.1007/s10753-014-9874-5
- Lopes de Faria, J. M., Duarte, D. A., Montemurro, C., Papadimitriou, A., Consonni, S. R., and Lopes de Faria, J. B. (2016). Defective Autophagy in Diabetic Retinopathy. *Invest. Ophthalmol. Vis. Sci.* 57 (10), 4356–4366. doi:10.1167/iovs.16-19197
- Mizushima, N., and Komatsu, M. (2011). Autophagy: Renovation of Cells and Tissues. *Cell* 147 (4), 728–741. doi:10.1016/j.cell.2011.10.026
- Ridano, M. E., Racca, A. C., Flores-Martin, J., Camolotto, S. A., de Potas, G. M., Genti-Raimondi, S., et al. (2012). Chlorpyrifos Modifies the Expression of

- Genes Involved in Human Placental Function. *Reprod. Toxicol. (Elmsford, N.Y.)*. 33 (3), 331–338. doi:10.1016/j.reprotox.2012.01.003
- Ridano, M. E., Subirada, P. V., Paz, M. C., Lorenc, V. E., Stupirski, J. C., Gramajo, A. L., et al. (2017). Galectin-1 Expression Imprints a Neurovascular Phenotype in Proliferative Retinopathies and Delineates Responses to Anti-VEGF. *Oncotarget* 8 (20), 32505–32522. doi:10.18632/oncotarget.17129
- Siman, R., Cocca, R., and Dong, Y. (2015). The mTOR Inhibitor Rapamycin Mitigates Perforant Pathway Neurodegeneration and Synapse Loss in a Mouse Model of Early-Stage Alzheimer-Type Tauopathy. *PLoS one* 10 (11), e0142340. doi:10.1371/journal.pone.0142340
- Shiba, T., Maeno, T., Saishin, Y., Hori, Y., and Takahashi, M. (2010). Nocturnal Intermittent Serious Hypoxia and Reoxygenation in Proliferative Diabetic Retinopathy Cases. *Am. J. Ophthalmol.* 149 (6), 959–963. doi:10.1016/j.ajo.2010.01.006
- Subirada, P. V., Paz, M. C., Ridano, M. E., Lorenc, V. E., Fader, C. M., Chiabrando, G. A., et al. (2019). Effect of Autophagy Modulators on Vascular, Glial, and Neuronal Alterations in the Oxygen-Induced Retinopathy Mouse Model. *Front. Cell. Neurosci.* 13, 279. doi:10.3389/fncel.2019.00279
- Subirada, P. V., Paz, M. C., Ridano, M. E., Lorenc, V. E., Vaglianti, M. V., Barcelona, P. F., et al. (2018). A Journey into the Retina: Müller Glia Commanding Survival and Death. *Eur. J. Neurosci.* 47 (12), 1429–1443. doi:10.1111/ejn.13965
- Szymanska, M., Mahmood, D., Yap, T. E., and Cordeiro, M. F. (2021). Recent Advancements in the Medical Treatment of Diabetic Retinal Disease. *Int. J. Mol. Sci.* 22 (17), 9441. doi:10.3390/ijms22179441
- Thomas, A., Belaidi, E., Moulin, S., Horman, S., van der Zon, G. C., Viollet, B., et al. (2017). Chronic Intermittent Hypoxia Impairs Insulin Sensitivity but Improves Whole-Body Glucose Tolerance by Activating Skeletal Muscle AMPK. *Diabetes* 66 (12), 2942–2951. doi:10.2337/db17-0186
- Wang, J., Xu, X., Elliott, M. H., Zhu, M., and Le, Y. Z. (2010). Müller Cell-Derived VEGF Is Essential for Diabetes-Induced Retinal Inflammation and Vascular Leakage. *Diabetes* 59 (9), 2297–2305. doi:10.2337/db09-1420
- Xin, X., Dang, H., Zhao, X., and Wang, H. (2017). Effects of Hypobaric Hypoxia on Rat Retina and Protective Response of Resveratrol to the Stress. *Int. J. Med. Sci.* 14 (10), 943–950. doi:10.7150/ijms.19391
- Yafai, Y., Lange, J., Wiedemann, P., Reichenbach, A., and Eichler, W. (2007). Pigment Epithelium-Derived Factor Acts as an Opponent of Growth-Stimulatory Factors in Retinal Glial-Endothelial Cell Interactions. *Glia* 55 (6), 642–651. doi:10.1002/glia.20495
- Yang, X. M., Yafai, Y., Wiedemann, P., Kuhrt, H., Wang, Y. S., Reichenbach, A., et al. (2012). Hypoxia-induced Upregulation of Pigment Epithelium-Derived Factor by Retinal Glial (Müller) Cells. *J. Neurosci. Res.* 90 (1), 257–266. doi:10.1002/jnr.22732
- Yuan, Y., Hilliard, G., Ferguson, T., and Millhorn, D. E. (2003). Cobalt inhibits the interaction between hypoxia-inducible factor- α and von Hippel-Lindau protein by direct binding to hypoxia-inducible factor- α . *J. Biol. Chem.* 278 (18), 15911–15916. doi:10.1074/jbc.M300463200
- Zhang, M. L., Zhao, G. L., Hou, Y., Zhong, S. M., Xu, L. J., Li, F., et al. (2020). Rac1 Conditional Deletion Attenuates Retinal Ganglion Cell Apoptosis by Accelerating Autophagic Flux in a Mouse Model of Chronic Ocular Hypertension. *Cel Death Dis.* 11 (9), 734. doi:10.1038/s41419-020-02951-7
- Zhou, J., Chen, F., Yan, A., and Xia, X. (2021). Role of Mammalian Target of Rapamycin in Regulating HIF-1 α and Vascular Endothelial Growth Factor Signals in Glaucoma. *Arch. Physiol. Biochem.* 127 (1), 44–50. doi:10.1080/13813455.2019.1609996
- Zhou, J., Huo, X., Botchway, B., Xu, L., Meng, X., Zhang, S., et al. (2018). Beneficial Effects of Resveratrol-Mediated Inhibition of the mTOR Pathway in Spinal Cord Injury. *Neural plasticity* 2018, 7513748. doi:10.1155/2018/7513748
- Zwanzig, A., Meng, J., Müller, H., Bürger, S., Schmidt, M., Pankonin, M., et al. (2021). Neuroprotective Effects of Glial Mediators in Interactions between Retinal Neurons and Müller Cells. *Exp. Eye Res.* 209, 108689. doi:10.1016/j.exer.2021.108689

Conflict of Interest: The authors declare that the research was conducted in the absence of any commercial or financial relationships that could be construed as a potential conflict of interest.

Publisher's Note: All claims expressed in this article are solely those of the authors and do not necessarily represent those of their affiliated organizations, or those of the publisher, the editors and the reviewers. Any product that may be evaluated in this article, or claim that may be made by its manufacturer, is not guaranteed or endorsed by the publisher.

Copyright © 2022 Subirada, Vaglianti, Joray, Paz, Barcelona and Sánchez. This is an open-access article distributed under the terms of the Creative Commons Attribution License (CC BY). The use, distribution or reproduction in other forums is permitted, provided the original author(s) and the copyright owner(s) are credited and that the original publication in this journal is cited, in accordance with accepted academic practice. No use, distribution or reproduction is permitted which does not comply with these terms.

NOMENCLATURE

ATG-5	Autophagy related protein 5	LC3B	Microtubule-associated proteins 1A/1B light chain 3B
BAECs	Bovine Aortic Endothelial Cells	MGCs	Müller glial cells
CoCl₂	Cobalt chloride	mTOR	mammalian target of Rapamycin
CQ	Chloroquine	MTT	3-[4,5-dimethylthiazol-2-yl]-2,5 diphenyl tetrazolium bromide
ECs	endothelial cells	O₂	Oxygen
Gal-1	Galectin-1	OIR	Oxygen-induced retinopathy
GFAP	Glial fibrillary acid protein	p62	sequestosome 1 (SQSTM 1)
HIF-1	Hypoxia inducible factor 1	PDR	proliferative diabetic retinopathy
		PEDF	pigment epithelium-derived factor
		VEGF	Vascular endothelial growth factor